



Article scientifique

Article

2006

Published version

Open Access

This is the published version of the publication, made available in accordance with the publisher's policy.

Recombinant expression and biochemical characterization of the unique elongating β -Ketoacyl-acyl carrier protein synthase involved in fatty acid biosynthesis of *Plasmodium falciparum* using natural and artificial substrates

Lack, Gabriela; Homberger-Zizzari, Eleonora; Folkers, Gerd; Scapozza, Leonardo; Perozzo, Remo

How to cite

LACK, Gabriela et al. Recombinant expression and biochemical characterization of the unique elongating β -Ketoacyl-acyl carrier protein synthase involved in fatty acid biosynthesis of *Plasmodium falciparum* using natural and artificial substrates. In: The Journal of biological chemistry, 2006, vol. 281, n° 14, p. 9538–9546. doi: 10.1074/jbc.M509119200

This publication URL: <https://archive-ouverte.unige.ch/unige:166439>

Publication DOI: [10.1074/jbc.M509119200](https://doi.org/10.1074/jbc.M509119200)

Recombinant Expression and Biochemical Characterization of the Unique Elongating β -Ketoacyl-Acyl Carrier Protein Synthase Involved in Fatty Acid Biosynthesis of *Plasmodium falciparum* Using Natural and Artificial Substrates*

Received for publication, August 18, 2005, and in revised form, January 11, 2006 Published, JBC Papers in Press, February 8, 2006, DOI 10.1074/jbc.M509119200

Gabriela Lack[‡], Eleonora Homberger-Zizzari[§], Gerd Folkers[¶], Leonardo Scapozza[‡], and Remo Perozzo^{‡1}

From the [‡]Pharmaceutical Biochemistry Group, School of Pharmaceutical Sciences, University of Geneva, University of Lausanne, Quai Ernest-Ansermet 30, CH-1211 Geneva 4, Switzerland, the [§]Department of Chemistry and Applied BioSciences, Swiss Federal Institute of Technology, Winterthurerstrasse 190, CH-8057 Zurich, Switzerland, and [¶]Collegium Helveticum, University of Zurich and Swiss Federal Institute of Technology, Schmelzbergstrasse 25, CH-8092 Zurich, Switzerland

The human malaria parasite *Plasmodium falciparum* synthesizes fatty acids by using a type II synthase that is structurally different from the type I system found in eukaryotes. Because of this difference and the vital role of fatty acids, the enzymes involved in fatty acid biosynthesis of *P. falciparum* represent interesting targets for the development of new antimalarial drugs. β -Ketoacyl-acyl carrier protein (ACP) synthase (PfFabBF), being the only elongating β -ketoacyl-ACP synthase in *P. falciparum*, is a potential candidate for inhibition. In this study we present the cloning, expression, purification, and characterization of PfFabBF. Soluble protein was obtained when PfFabBF was expressed as a NusA fusion protein in *Escherichia coli* BL21(DE3)-CodonPlus-RIL cells under conditions of osmotic stress. The fusion protein was purified by affinity and ion exchange chromatography. Various acyl-*P. falciparum* acyl carrier protein (PfACP) substrates were tested for their specific activities, and their kinetic parameters were determined. Activity of PfFabBF was highest with C_{4:0}- to C_{10:0}-acyl-PfACPs and decreased with use of longer chain acyl-PfACPs. Consistent with the fatty acid synthesis profile found in the parasite cell, no activity could be detected with C_{16:0}-PfACP, indicating that the enzyme is lacking the capability of elongating acyl chains that are longer than 14 carbon atoms. PfFabBF was found to be specific for acyl-PfACPs, and it displayed much lower activities with the corresponding acyl-CoAs. Furthermore, PfFabBF was shown to be sensitive to cerulenin and thiolactomycin, known inhibitors of β -ketoacyl-ACP synthases. These results represent an important step toward the evaluation of *P. falciparum* β -ketoacyl-ACP synthase as a novel antimalaria target.

Malaria is one of the world's most important infectious diseases in terms of both mortality and morbidity. The consensus is that 0.5 billion clinical attacks take place every year, including 2–3 million severe attacks (1–3). It is assumed that the disease claims more than 1 million lives annually and that most of these deaths occur in African children, but the true number might be much higher. Chloroquine, which used to be the first line treatment for malaria, now fails everywhere. Emerging

resistance to drugs introduced to replace chloroquine, such as sulfadoxine-pyrimethamine, reinforces the need for new, selective, and affordable drugs against the parasite (1). Of the four causative agents of malaria, i.e. *Plasmodium falciparum*, *Plasmodium vivax*, *Plasmodium ovale*, and *Plasmodium malariae*, *P. falciparum* is the most dangerous. The recent completion of the genome sequencing of *P. falciparum* allowed the identification of highly promising pathways in the parasite (4). One of the most interesting discoveries was the presence of a complete type II fatty acid biosynthesis pathway (FAS²-II) (5, 6). FAS-II is found in bacteria and plants and is structurally very different from the FAS-I system found in most eukaryotes. In FAS-I, the biosynthetic enzymes are integrated into a large multifunctional single polypeptide (7), whereas FAS-II uses separate, discrete enzymes that carry out the individual steps during initiation and chain elongation (8).

The importance of lipids for parasite survival has generated much interest in the enzymes responsible for their biosynthesis. Their inhibition has been shown repeatedly to be a suitable target for antimicrobials (9). Thus, the intervention at the level of *P. falciparum* FAS-II represents a very promising approach for the development of new antimalarials (10, 11).

Among the inhibitors described to act against various targets in FAS-I and FAS-II, thiolactomycin and cerulenin are known to inhibit the β -ketoacyl-ACP synthases FabB and FabF of bacteria (e.g. *Escherichia coli* and *Mycobacterium tuberculosis*) and plants (e.g. *Pisum sativum* and *Allium porrum*) (12–17). Cerulenin inactivates the enzymes irreversibly, forming a covalent adduct with the active site cysteine (14). Thiolactomycin is a reversible inhibitor that competes with malonyl-ACP for binding (16–21). β -Ketoacyl-ACP synthases catalyze the Claisen condensation reaction, transferring an acyl primer to malonyl-ACP and thereby creating a β -ketoacyl-ACP product that has been lengthened by a two-carbon unit. In the type II FAS of plants and bacteria, three β -ketoacyl-ACP synthases with different substrate specificities have emerged as important regulators of the initiation and elongation steps in the pathway. The initiation enzyme β -ketoacyl synthase III (FabH) only catalyzes the elongation of malonyl-ACP by an acetyl-CoA primer, whereas the elongation enzymes β -ketoacyl synthase I and II (FabB and FabF) use acyl-ACPs for elongation of malonyl-ACP (18).

* This work was supported by the Novartis Foundation (formerly the Ciba-Geigy Jubilee Foundation). The costs of publication of this article were defrayed in part by the payment of page charges. This article must therefore be hereby marked "advertisement" in accordance with 18 U.S.C. Section 1734 solely to indicate this fact.

¹ To whom correspondence should be addressed: Biochimie Pharmaceutique, Laboratoire de Chimie Thérapeutique, Section des Sciences Pharmaceutiques, Université de Genève, Quai Ernest-Ansermet 30, CH-1211 Genève 4, Switzerland. Tel.: 41-22-3793371; Fax: 41-22-3793360; E-mail: remo.perozzo@pharm.unige.ch.

² The abbreviations used are: FAS, fatty-acid synthase; PfACP, *P. falciparum* acyl carrier protein; EcACPS, *E. coli* holo-acyl carrier protein synthase; PfFabBF, *P. falciparum* β -ketoacyl-ACP synthase; PfFabG, *P. falciparum* β -ketoacyl-ACP reductase; DTT, dithiothreitol; CER, cerulenin; TLM, thiolactomycin; TB, terrific broth; CS-PAGE, conformational sensitive gel electrophoresis; BisTris, 2-[bis(2-hydroxyethyl)amino]-2-(hydroxymethyl)propane-1,3-diol.

Sequencing of the full genome of *P. falciparum* revealed that the parasite possesses only one isoform of the elongating condensing enzyme, PfFabBF. As PfFabBF is unique, its activity cannot be replaced by another β -ketoacyl-ACP synthase, which makes it a very promising target. To date there are no data available concerning substrate specificity and kinetic parameters of PfFabBF. To this end, we present the cloning, expression, and purification of this enzyme. A recombinant expression and purification system was established, allowing the production of significant amounts of active enzyme that are suitable for the characterization using natural acyl-PfACP substrates as well as the corresponding acyl-CoA analogs.

EXPERIMENTAL PROCEDURES

Materials and Instrumentation—All cloning steps were performed in *E. coli* Nova Blue cells (Stratagene). Expression was conducted in *E. coli* BL21(DE3)-CodonPlus-RIL cells (Stratagene). Sources of supplies are as follows: pET vectors from Novagen; *Pfu* Turbo polymerase from Stratagene; T4 DNA ligase and restriction enzymes from New England Biolabs; plasmid extraction kits from Sigma; NADPH from Roche Diagnostics; Terrific broth (TB) medium from Difco; cerulenin and acyl-CoAs from Sigma; nickel-nitrilotriacetic acid-agarose from Qiagen; HiTrap, HisTrap, PD10 and Superdex 75/200 gel filtration columns from Amersham Biosciences. An Aekta FPLC (Amersham Biosciences) was used for protein purification. Spectrophotometric measurements were carried out on a Cary 50 concentration Varian Spectrophotometer using an ultra-micro cell from Hellma (type 105.202-QS). All other supplies were reagent grade or better.

Multiple Sequence Alignment—Sequences of β -ketoacyl-ACP synthases of various organisms were aligned using the ClustalW alignment program (22). The sequences were obtained from the SwissProt data base and included *E. coli* FabB (SwissProt primary accession number P14926) and FabF (P39435), *Arabidopsis thaliana* FabB (P52410) and FabF (Q9C9P4), and *P. falciparum* FabBF (Q6LF11).

Cloning of the *P. falciparum* PfFabBF Expression Plasmids—A two-step megaprimer PCR method (23, 24) was used to create a *pfabBF* clone that carried a 171-bp truncation at the N terminus. In the first step, two overlapping fragments of the *pfabBF* gene were PCR-amplified from *P. falciparum* 3D7 gDNA (MRA-386, MR4; ATCC, Manassas VA). The first fragment was amplified using the forward primer 5'-ACTTCTAGAGTGGTGTGCACAG and the reverse primer 5'-CCTGAACCTTCTCCCATAACGAAACCACACG. The second fragment was generated using the following primer pair: 5'-GAAGTGTTTCGTTATGGGAGAAGGTTTCAGG and 5'-TCACTTTACAATTTTTTTGAAAAGTAATG. In a second step, the above mentioned fragments were combined to give the final insert using forward primer 5'-TGGTTCATGGCTTCTAGAGTGGTGTGCACAGGTGTAGGGTA and reverse primer 5'-CCGAATTCACATTTACAATTTTTTGAAAAGTAATGCTGTGTTATGGCCTCC who carried NcoI and EcoRI restriction sites, respectively (underlined). The PCR program for both reactions consisted of an initial 2-min denaturation step (94 °C), followed by 25 cycles of 94 °C for 30 s, 45 °C for 30 s, 48 °C for 90 s, and 60 °C for 60 s, followed by a final elongation step at 60 °C for 5 min. The amplified gene was digested with NcoI and EcoRI and ligated into pET30b vector using T4 DNA ligase.

An 18-bp-long stretch of DNA, coding for six additional amino acids (*i.e.* KNLCE^T) of the original *pfabBF* N terminus, was introduced by site-directed mutagenesis using as template the plasmid described above. The following primers were used: 5'-GGTACCGACGACGACGACAAGCATATGAAAAATCTTTGTGAAACTTCTAGAGTGGTGTGCACAGGTGTAGGGGT and 5'-ACCCCTACACCTGTGCA-

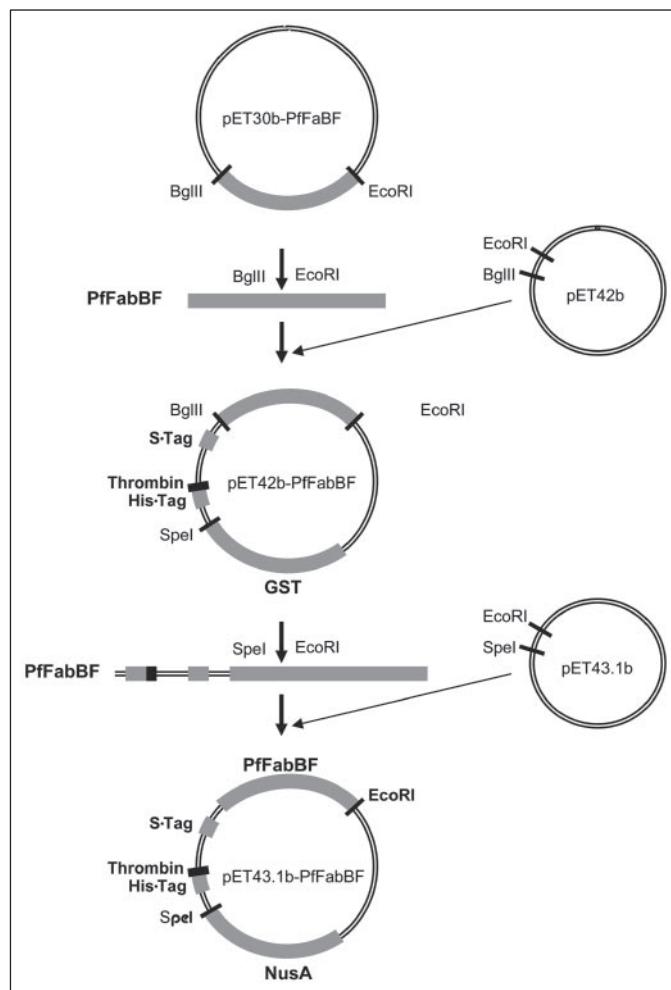


FIGURE 1. Construction of the PfFabBF expression vector. pET30b-PfFabBF was digested with BglII and EcoRI, and the resulting fragment was subcloned into an equally digested pET42b vector. Cleavage with SpeI and EcoRI generated a fragment that contained the whole PfFabBF open reading frame, including a His tag as well as an S tag, which was inserted into a pET43.1b vector to give the final pET43.1b-PfFabBF expression plasmid.

CACCACTCTAGAAGTTTCACAAAGATTTTTTCATATGCTTGTCGTCGTCGTCGGTACC. The amplification was carried out with *Pfu* Turbo polymerase. The PCR program consisted of a 2-min initial denaturation step at 94 °C, followed by 18 cycles of 95 °C for 50 s, 48 °C for 60 s, 52 °C for 60 s, and 68 °C for 14 min, and a final polishing step at 68 °C for 7 min. The original plasmid was digested with DpnI at 37 °C for 90 min. The remaining mutated plasmid was purified by ethanol precipitation and used to transform CaCl₂ competent Nova Blue *E. coli* cells. Positive mutants were identified by sequencing.

This elongated construct was named pET30b-PfFabBF and was used for all further subcloning steps. pET30b-PfFabBF was digested with BglII and EcoRI and ligated into an equally digested pET42b vector. The resulting pET42b-PfFabBF was then digested with SpeI and EcoRI and ligated into pET43.1b to give pET43.1b-PfFabBF (Fig. 1). All positive clones were identified by PCR screening, restriction digestion, and automated sequencing to verify authenticity.

Expression and Purification of PfFabBF—The final pET43.1b-PfFabBF clone was designed to express PfFabBF as NusA fusion protein with an expected molecular mass of 107 kDa, covering amino acids 52–474 of the β -ketoacyl-ACP synthase part. The expression plasmid was introduced into BL21(DE3)-CodonPlus-RIL expression cells. The cells were used to inoculate 500 ml of TB medium supplemented with 1

β -Ketoacyl-ACP Synthase from *P. falciparum*

mM betaine, 660 mM sorbitol, ampicillin (100 μ g/ml), and chloramphenicol (34 μ g/ml) and grown overnight at 37 °C. The temperature was then lowered to 25 °C, and protein production was induced with 1 mM isopropyl β -D-thiogalactopyranoside for 7 h. The cells were harvested by centrifugation, resuspended in lysis buffer (20 mM NaH_2PO_4 , 500 mM NaCl, 20 mM imidazole, 2 mM DTT, 10% glycerol, pH 7.5) containing DNase, and disrupted by passing them twice through a French press. The extract was clarified, and the supernatant was applied to a 5-ml HisTrap chelating column. The column was washed with 4 column volumes of lysis buffer and eluted by means of a 50-ml linear imidazole gradient using buffer A (20 mM NaH_2PO_4 , 500 mM NaCl, 2 mM DTT, 10% glycerol, pH 7.5) and buffer B (20 mM NaH_2PO_4 , 500 mM NaCl, 500 mM imidazole, 2 mM DTT, 10% glycerol, pH 7.5). Fractions containing PfFabBF were pooled, concentrated (Centriprep, 30-kDa cut-off), diluted to a final NaCl concentration of 50 mM, and loaded on a 5-ml HiTrap SP-Sepharose HP column. The protein was eluted with a linear NaCl gradient using buffer C (20 mM NaH_2PO_4 , 2 mM DTT, pH 7.5) and buffer D (20 mM NaH_2PO_4 , 1 M NaCl, 2 mM DTT, pH 7.5). The fractions containing the fusion protein were again pooled, concentrated, and either applied on a Superdex 200 column equilibrated with buffer E (20 mM NaH_2PO_4 , 300 mM NaCl, 2 mM DTT, 10% glycerol, pH 7.5) or desalted by ultrafiltration (Amicon Ultra 4, 30-kDa cut-off), depending on the required degree of purity. Total protein concentration was determined by a dye-binding assay (25). The purified protein was stored at +4 °C.

Cloning and Expression of *P. falciparum* ACP—Acyl-PfACPs are the natural substrates of PfFabBF and are thus needed for its characterization. PfACP has been cloned and expressed in a similar way as described earlier (26, 27). Briefly, the *pfacp* gene sequence N-terminally truncated by 180 bp was PCR-amplified from a *P. falciparum* strain 3D7 gametocyte stage cDNA pSPORT plasmid library (kindly provided by Dr. T. Templeton, Weill Medical College of Cornell University) and ligated into the pET28b expression vector. Correct clones were identified and verified by restriction digestion, PCR, and automated sequencing with T7 forward and reverse primers. The resulting clone was designed to express PfACP without the putative N-terminal signal and translocation sequence, *i.e.* amino acids 1–60. PfACP, consisting of residues 61–137, was expressed for 8 h at 37 °C in TB medium supplemented with kanamycin (100 μ g/ml) and chloramphenicol (34 μ g/ml) using BL21(DE3)-CodonPlus-RIL expression cells. After isolation on a HisTrap chelating column and subsequent imidazole gradient elution, the N-terminal His tag was removed by thrombin digestion. The protein was concentrated, diluted in buffer A (20 mM BisTris, pH 6.5) to a final NaCl concentration of 50 mM, and applied to a 5-ml HiTrap Q-Sepharose XL column in order to separate the apo-form of the protein from the holo-form. Apo-PfACP and holo-PfACP were separated by applying a linear NaCl gradient (120 ml) using buffer A and buffer B (20 mM BisTris, 1 M NaCl, pH 6.5). Fractions containing apo-PfACP were pooled and reapplied to the column. Three runs were necessary to complete the separation. The purity of apo-PfACP was verified by conformational sensitive gel electrophoresis (CS-PAGE) (28, 29). The pure fractions were concentrated (Centriprep, 3-kDa cut-off) and stored at –20 °C.

Cloning and Expression of *E. coli* ACPS—In order to produce the acyl-PfACPs enzymatically, EcACPS has been cloned and expressed essentially as described earlier (30). Briefly, the complete *acpS* coding sequence was amplified from *E. coli* genomic DNA and ligated into the pET30b expression vector. Correct clones were identified and verified by restriction digestion, PCR, and automated sequencing with T7 forward and reverse primers. The resulting plasmid was introduced into BL21(DE3)-CodonPlus-RIL expression cells, and the protein was expressed

for 8 h at 37 °C in TB medium supplemented with kanamycin (100 μ g/ml) and chloramphenicol (34 μ g/ml). After isolation on a HisTrap chelating column and subsequent imidazole gradient elution, EcACPS was desalted by applying the concentrated fractions to a PD10 column. The protein was eluted with a buffer containing 20 mM Tris, pH 8.0, 150 mM NaCl, 10% glycerol, and 3 mM DTT.

Cloning, Expression, and Purification of PfFabG—Activity assays of PfFabBF were performed by coupling the synthase activity of PfFabBF to the reductase activity of PfFabG. A *pfabG* sequence N-terminally truncated by 162 bp was PCR-amplified from a *P. falciparum* (strain 3D7) gametocyte cDNA pSPORT plasmid library and after restriction digestion was ligated into the pET30b expression vector. Correct clones were identified and verified by restriction digestion, PCR, and automated sequencing with T7 forward and reverse primers. The resulting clone was designed to express the enzyme without the putative N-terminal signal and translocation sequence, *i.e.* amino acids 1–54. PfFabG, consisting of residues 55–304, was expressed for 6 h at 37 °C using BL21(DE3)-CodonPlus-RIL cells. Purification of the protein was performed as described for PfFabI (31), except that a linear imidazole gradient was applied.

Preparation of Acylated PfACP Substrates— $C_{4:0}$ to $C_{16:0}$ acyl-PfACPs were generated using EcACPS. A typical reaction (1 ml) contained 100 μ M of the corresponding acyl-CoA, 250 μ g of EcACPS, 1 mg of apo-PfACP, 25 mM MgCl_2 in 20 mM Tris, pH 7.5. For higher amounts of substrates, the protocol was scaled up accordingly. The mixture was incubated at 37 °C for 1 h. EcACPS was eliminated from the mixture by binding it to nickel-nitrilotriacetic acid-agarose. Afterward the acyl-PfACPs were concentrated and desalted by means of a PD10 column equilibrated with 20 mM NaH_2PO_4 and 300 mM NaCl, pH 7.5. The purity of acyl-PfACPs was confirmed by CS-PAGE (28, 29).

Enzyme Assays—A continuous assay format was used to monitor the PfFabBF activity by coupling the condensing activity of PfFabBF to PfFabG. FabG reduces β -ketoacyl-ACPs to the corresponding β -hydroxyacyl-ACPs by simultaneous oxidation of its cofactor NADPH to NADP^+ , allowing the reaction course to be monitored spectrophotometrically at 340 nm. Control experiments, such as performing the reaction either without substrates or without enzyme, were carried out to rule out unspecific oxidase activity.

Specific activity measurements of the acyl-PfACPs were performed at 37 °C and contained 30 μ M malonyl-PfACP, 30 μ M acyl-PfACP (1 mM for the acyl-CoA series), and 5 μ g of PfFabG in assay buffer (20 mM NaH_2PO_4 , 300 mM NaCl, 80 μ M NADPH, 1 mM DTT, pH 7.5) in a total volume of 100 μ l. The reaction was started with the addition of 3 μ g of PfFabBF. The course of the reaction was monitored for 1 min, and the rates of product formation were expressed as pmol/min. The substrate specificity of PfFabBF was additionally checked by CS-PAGE in order to exclude the possibility of PfFabG being the limiting factor.

Kinetic measurements were performed with $C_{4:0}$ - to $C_{14:0}$ -PfACPs under Michaelis-Menten conditions at 37 °C using various concentrations of acyl-PfACP (25, 50, 100, 200, 300, 400, 500, 600, and 800 μ M), malonyl-PfACP at saturating conditions (400 μ M), and 5 μ g of PfFabG in assay buffer (final volume 100 μ l). The kinetic parameters of malonyl-PfACP were determined using 500 μ M $C_{4:0}$ -PfACP and various concentrations of malonyl-PfACP (6.25, 12.5, 25, 50, 100, 200, and 400 μ M). The reaction was started with the addition of 3 μ g of PfFabBF. Control experiments (*e.g.* linearity of the rate of product formation at different PfFabBF concentrations) were performed to show that PfFabG is not the rate-limiting step in the reaction.

Cerulenin Inhibition Assay—Time dependence of cerulenin (CER) inhibition was analyzed by adding 3 μ g of PfFabBF that had been pre-

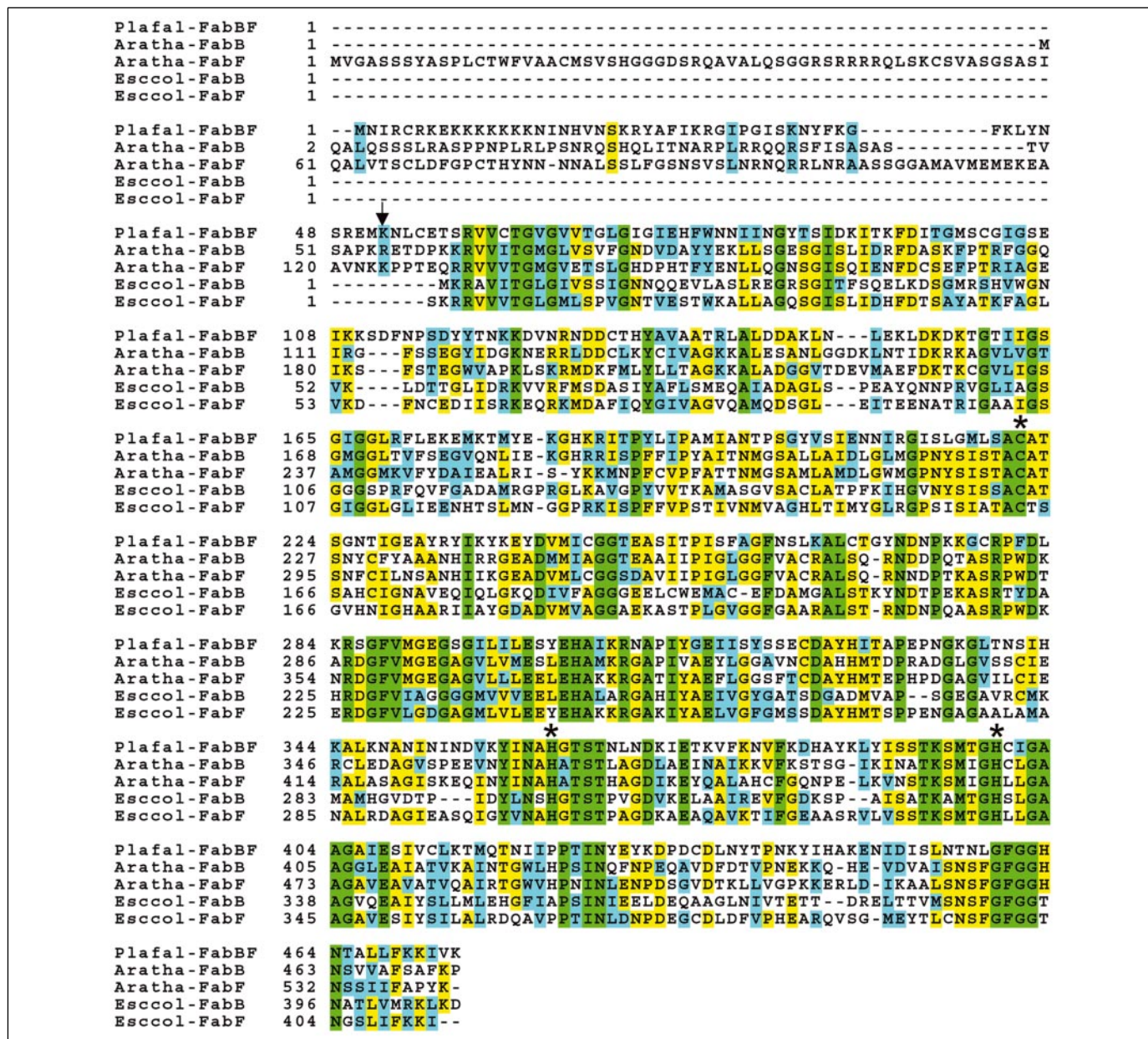


FIGURE 2. Multiple sequence alignment of PfFabBF with FabB and FabF of *E. coli* and *A. thaliana*, respectively. Green indicates completely conserved residues; yellow indicates three or more highly conserved residues; blue indicates at least one similar amino acid residue. The first residue of the expressed protein, Lys-52, is marked with an arrow, and the catalytically important residues Cys-221, His-362, and His-399 are marked with asterisks.

incubated with 100 μ M CER for 0, 10, 15, 20, 30, 45, 60, and 120 s to the assay buffer containing 30 μ M malonyl-PfACP, 30 μ M hexanoyl-PfACP, and 5 μ g of PfFabG (total volume 100 μ l). The IC₅₀ value was determined using various concentrations of CER (0, 1, 10, 25, 50, and 100 μ M) in the reaction mixture described above. The reaction was started without preincubation by the addition of 3 μ g of enzyme. The irreversibility of CER inhibition was confirmed by adding inhibited enzyme to the reaction mixture described above, thereby diluting the CER concentration 20-fold. All measurements were performed at 37 °C.

Thiolactomycin Inhibition Assay—The IC₅₀ value was determined as described for CER, except that the following thiolactomycin (TLM) concentrations were used: 0, 1, 10, 50, and 100 μ M. The type of inhibition was determined with respect to malonyl-PfACP and C_{6:0}-PfACP in consideration of the Michaelis-Menten steady state condition. To investigate the inhibition mechanism of TLM with respect to malonyl-

PfACP, 250 μ M C_{6:0}-PfACP, various concentrations of malonyl-PfACP (10, 25, 50, 100, and 200 μ M), and 1 μ g of PfFabG were added to the assay buffer. The reaction was started by the addition of 3 μ g of PfFabBF. The type of inhibition with respect to acyl-PfACP was determined as described for malonyl-PfACP, except that the C_{6:0}-PfACP concentration was varied (50, 100, 200, 400, and 500 μ M), and the malonyl-PfACP concentration was kept constant at 400 μ M.

RESULTS

The fatty acid biosynthesis of *P. falciparum* received considerable attention with the recent discovery of this pathway in the parasite. In the meantime several key enzymes involved have been characterized with respect to their biochemical behavior as well as to their three-dimensional structure, and first inhibitors have been found or designed. However, the enzymatic characteristics of the β -ketoacyl-ACP synthase I/II

β -Ketoacyl-ACP Synthase from *P. falciparum*

homolog of the *P. falciparum* pathway have not been reported yet in the literature. The Plasmodium Genome Data base (32) proposed the open reading frame PFF1275c to be the mentioned β -ketoacyl-ACP synthase (PfFabBF). To confirm this hypothesis, we cloned the cDNA corresponding to PFF1275c and characterized its gene product PfFabBF.

Multiple Sequence Alignment—The open reading frame encodes a protein of 474 amino acids with an expected molecular mass of 52.6 kDa. PfFabBF has a long N-terminal extension that is characteristic of bipartite N-terminal presequences found in *Plasmodium* and *Toxoplasma* parasite proteins targeted to the apicoplast (5, 33). The size of the adjacent apicoplast translocation signal cannot be predicted and remains to be determined experimentally. A multiple sequence alignment of PfFabBF with FabB and FabF of *E. coli* and *A. thaliana* is shown in Fig. 2. When compared with PfFabBF (residues 56–474), the parasite enzyme shares 31 and 38% identity with FabB (residues 1–406) and FabF (residues 1–412) of *E. coli* and 38 and 37% identity with FabB (residues 59–473) and FabF (residues 128–541) of *A. thaliana*. The typical Cys/His/His motif found in β -ketoacyl-ACP synthases is also present in PfFabBF. This group entails the active site cysteine and histidines that are involved in the elongation reaction. In PfFabBF they correspond to Cys-221, His-362, and His-399 (Fig. 2).

Expression and Purification of FabBF—Because of the lack of knowledge about the mature size of PfFabBF, the initial pET30b expression construct was designed to express a truncated enzyme missing the potential signal and translocation sequences, but retaining all amino acids needed to ensure complete functionality as deduced from sequence alignments with bacterial homologs. This initial pET30b vector containing the truncated *pfabBF* gene resulted in large quantities of protein that remained insoluble under any conditions. Subsequent refolding attempts achieved some solubilization, but the enzyme failed the activity tests, and it was shown by means of circular dichroism that it lacked secondary structure. At this stage a new clone (pET30b-Pf-fabBF) was prepared by site-directed mutagenesis to add back 6 amino acids derived from the N terminus that had been omitted in the first construct. Starting from this new construct, the extended insert was introduced into several pET vectors, aiming at the expression of the target protein with highly soluble fusion partners, *i.e.* glutathione *S*-transferase, thioredoxin, DsbA, and NusA. Only pET43.1b, which allows expression of the protein fused to the highly soluble NusA protein, resulted in a significant increase of soluble PfFabBF. The production of soluble fusion protein could be raised to acceptable amounts by subjecting the cells to osmotic stress (34, 35). We supplemented the TB medium with 1 mM betaine and sorbitol. Of all sorbitol concentrations tested (0, 330, and 660 mM and 1 M), 660 mM gave the best result. The identity of the fusion protein was confirmed by SDS-PAGE (Fig. 3A), Western blotting, and thrombin digestion. The first purification step of the fusion protein consisted of loading the clarified soluble fraction on a HisTrap chelating column. NusA-fusion proteins from pET43 are known to bind rather weakly to the nickel column, making a complete elimination of contaminating proteins difficult. PfFabBF eluted at an imidazole concentration of 125 mM and was of low purity, as expected. Most contaminants were eliminated by cation exchange chromatography, resulting in a preparation of about 80% purity as deduced from SDS-PAGE and gel densitometry. A final polishing step using gel filtration chromatography could increase purity to >95% but resulted in >50% loss of protein. Various control experiments showed clearly that the impurities present in the sample do not interfere with the measurement (*i.e.* do not introduce unspecific oxidase activity). In addition, the NusA-PfFabBF fusion protein displayed identical activities compared with the thrombin-cleaved PfFabBF. Based on these results, we used the

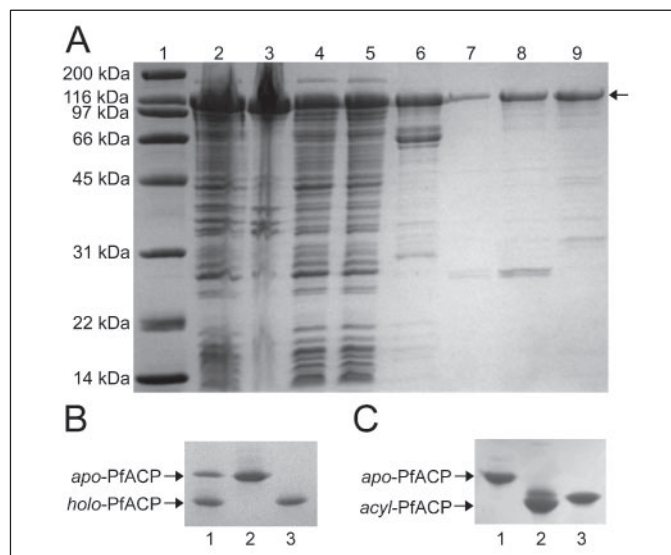


FIGURE 3. PAGE analysis of PfFabBF purification and acyl-PfACP preparation. A, samples were run on 12% SDS gels in Tris-SDS buffer. PfFabBF eluted between 125 and 275 mM imidazole. The band corresponding to the fusion protein (107 kDa) is marked with an arrow. Lane 1, broad range marker; lane 2, crude extract; lane 3, insoluble fraction; lane 4, soluble fraction; lane 5, nickel column flow-through; lane 6, nickel column eluate; lanes 7–9, SP-Sepharose HP column elution fractions. B, the three forms of PfACP (apo, holo, and acyl) were separated and analyzed by CS-PAGE using 5 M urea in 15% polyacrylamide gels. The corresponding bands are indicated by arrows. Lane 1, apo- and holo-PfACP after thrombin digestion; lane 2, pure apo-PfACP after ion exchange chromatography; lane 3, holo-PfACP removed after ion exchange chromatography. C, CS-PAGE analysis of PfACP acylation. Lane 1, apo-PfACP before acylation; lane 2, pure malonyl-ACP which migrates as two bands; lane 3, $C_{4:0}$ -ACP as a representative of $C_{4:0}$ to $C_{16:0}$ -PfACP, all of which exhibiting identical migration behavior.

more stable fusion protein for all measurements. The purification typically resulted in 2–3 mg of PfFabBF fusion protein/liter of media.

Purification of PfACP and Preparation of Acylated Substrates—Expression of PfACP in BL21(DE3)-CodonPlus-RIL cells and subsequent purification by nickel affinity chromatography yielded 20–30 mg of highly pure protein/liter culture. Thrombin-digested apo- and holo-PfACP were separated by anion exchange chromatography (Fig. 3B). Pure apo-PfACP was used for acylation by EcACPS. Under the experimental conditions described, the acylation of PfACP is complete within 2 min when acyl-CoAs with chain lengths up to $C_{14:0}$ were used. The reaction was considerably slower with $C_{16:0}$ -CoA; thus the incubation time was extended to 1 h to ensure complete acylation. Purity of the acyl-PfACPs was verified by matrix-assisted laser desorption ionization time-of-flight-mass spectrometry and by CS-PAGE (Fig. 3C).

PfFabBF Activity with Acyl-PfACP and Acyl-CoA as Substrates—To examine the substrate acceptance, we tested $C_{4:0}$ to $C_{16:0}$ -acyl-PfACPs and the corresponding acyl-CoAs. PfFabBF readily elongates $C_{4:0}$ through $C_{10:0}$ -PfACPs, has significantly less activity with $C_{12:0}$ - and $C_{14:0}$ -PfACPs, and no capacity for elongation of $C_{16:0}$ -PfACP (Table 1). The acyl-CoAs are much poorer substrates compared with acyl-PfACPs. When measured at 30 μ M, the activity of PfFabBF with $C_{4:0}$ to $C_{14:0}$ -CoAs as substrates was in the range of the background, but a trend toward higher activity with $C_{16:0}$ - and $C_{18:0}$ -CoAs could be observed. At acyl-CoA concentrations of 1 mM we detected activity with $C_{4:0}$ to $C_{14:0}$ -CoAs. PfFabBF was found to be more than twice as active with $C_{16:0}$ - and $C_{18:0}$ -CoAs compared with the shorter chain acyl-CoAs (Table 1). Thus PfFabBF accepts long chain acyl-CoAs but not long chain acyl-PfACPs, and the long chain acyl-CoAs seem to be better substrates than the shorter chain acyl-CoAs.

Kinetic Parameters of PfFabBF Substrates—Kinetic parameters were determined for $C_{4:0}$ to $C_{14:0}$ - and malonyl-PfACP (Fig. 4A). The K_m

TABLE 1
PffabBF activity with acyl-PfACP and acyl-CoA substrates

Substrate ^a	Activity ^b
	pmol/min/μg
C _{4:0} -PfACP (CoA)	94.8 ± 6.6 (36.0 ± 10.9)
C _{6:0} -PfACP (CoA)	104.9 ± 9.1 (23.7 ± 4.3)
C _{8:0} -PfACP (CoA)	66.8 ± 1.4 (36.8 ± 3)
C _{10:0} -PfACP (CoA)	97.5 ± 9.7 (36.6 ± 7.6)
C _{12:0} -PfACP (CoA)	30.7 ± 4.2 (15.2 ± 9.2)
C _{14:0} -PfACP (CoA)	24.0 ± 0.6 (26.7 ± 17.3)
C _{16:0} -PfACP (CoA)	NDA ^c (100.0 ± 20.2)
C _{18:0} -PfACP (CoA)	ND ^d (88.8 ± 14.6)

^a Acyl-PfACP substrates are measured at 30 μM, and 1 mM of the corresponding CoA derivatives (shown in parentheses) is applied.

^b The activity towards the corresponding CoA substrates is shown in parentheses. The results are the mean of duplicate experiments.

^c NDA indicates no detectable activity.

^d ND indicates not determined.

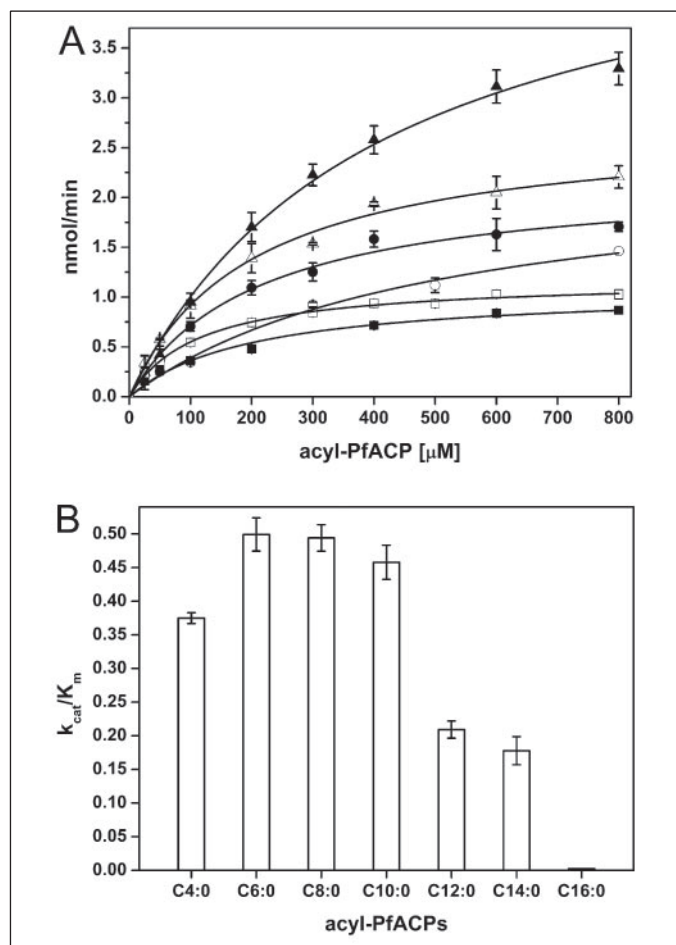


FIGURE 4. Kinetic analysis of PffabBF with acyl-PfACPs. A, the initial velocities of product formation were determined with increasing concentrations of acyl-PfACP. The data were analyzed by nonlinear regression analysis (Michaelis-Menten model) using Origin[®] software. The average of two data points has been plotted. ▲, C_{10:0}-PfACP; △, C_{8:0}-PfACP; ●, C_{4:0}-PfACP; ○, C_{14:0}-PfACP; ■, C_{6:0}-PfACP; □, C_{12:0}-PfACP. B, the catalytic efficiency of PffabBF for C_{4:0}- to C_{16:0}-PfACP was calculated from k_{cat} and K_m values. PffabBF exhibits maximum activity with C_{6:0}- to C_{10:0}-PfACP as substrates. The results reflect the mean of duplicate experiments.

values of the C_{4:0}- to C_{14:0}-PfACPs range from 115.6 to 437 μM, and the V_{max} values range from 1.2 to 5.2 nmol/min. For malonyl-PfACP, a K_m of 17.8 μM was found with respect to C_{4:0}-PfACP. The k_{cat}/K_m values for C_{4:0}- to C_{10:0}-PfACP range from 0.37 to 0.50 μM⁻¹ min⁻¹ (see Table 2). The values obtained for C_{12:0} and C_{14:0} are considerably lower, exhibiting decreased catalytic efficiencies by 40–50% (Fig. 4B). These kinetic results corroborate the findings obtained at the PffabBF activity test

TABLE 2
Kinetic parameters of acyl-PfACPs

Substrate	K_m	V_{max}	k_{cat}	k_{cat}/K_m
	μM	nmol/min	min ⁻¹	μM ⁻¹ min ⁻¹
C _{4:0} -PfACP	211.1 ± 9.9	2.2 ± 0.06	79.1 ± 2.0	0.37 ± 0.01
C _{6:0} -PfACP	115.6 ± 8.8	1.2 ± 0.03	57.6 ± 1.5	0.50 ± 0.02
C _{8:0} -PfACP	198.2 ± 11.6	2.7 ± 0.05	97.8 ± 1.9	0.49 ± 0.02
C _{10:0} -PfACP	403.4 ± 53.6	5.2 ± 0.40	184.0 ± 14.3	0.46 ± 0.03
C _{12:0} -PfACP	196.4 ± 5.5	1.2 ± 0.10	41.1 ± 3.6	0.21 ± 0.01
C _{14:0} -PfACP	437.0 ± 91.2	2.2 ± 0.20	76.7 ± 7.1	0.18 ± 0.02
C _{16:0} -PfACP	NDA ^a	NDA	NDA	NDA

^a NDA indicates no detectable activity.

described above, despite the limited informational content of measurements performed at single substrate concentrations.

Effects of CER and TLM on PffabBF—CER is known to be an irreversible inhibitor of *β*-ketoacyl-ACP synthases. To investigate the sensitivity of PffabBF to CER, the enzyme was preincubated with 100 μM CER. Samples were taken at various time points and assayed for activity. As expected, CER was found to be a potent inhibitor of PffabBF activity, leading to a complete inactivation of the enzyme within 1 min (Fig. 5A). The irreversibility of CER inhibition was confirmed by diluting the CER concentration 20-fold. In case of a reversible inhibitor, the enzyme would have regained activity. This was not the case with CER as the enzyme remained inactive. Because CER binds covalently to PffabBF, Fig. 5B reflects the rate of complex formation at different inhibitor concentrations. The IC₅₀ value was determined to be 15.8 ± 2.3 μM under the conditions applied.

TLM inhibits PffabBF reversibly with an IC₅₀ of 23.6 ± 6.0 μM (Fig. 6A). TLM is a competitive inhibitor with respect to malonyl-PfACP (Fig. 6B). Preliminary experiments indicate uncompetitive inhibition with respect to acyl-PfACP (data not shown). Analysis of the data according to Dixon and secondary plots resulted in a K_i value of 10 ± 4 μM.

DISCUSSION

In contrast to most other eukaryotes, Plasmodia harbor a type II fatty acid biosynthesis pathway. Because of structural differences to the eukaryotic system, the enzymes of FAS-II represent interesting new targets for the development of novel antimalarials. The unique elongation condensing enzyme in *P. falciparum*, PffabBF, is representative of these promising targets.

Multiple sequence alignments of PffabBF with *β*-ketoacyl-ACP synthases of other organisms display the homology of the enzymes, with 30–40% identical amino acids. As PffabBF is the unique elongating *β*-ketoacyl-ACP synthase in the pathway, it is of interest whether the enzyme could be annotated as either FabB- or FabF-type synthase. Comparison of PffabBF with plant FabB and FabF of *A. thaliana* disclosed very similar identity (38%) toward both enzymes, and it was not possible to distinguish between the two isoforms. The situation is different for *E. coli* FabB and FabF. Here the plasmodial enzyme shows more identity to FabF (31 versus 38%). This would be in line with the general assumption that FabF is the “generic” synthase, whereas FabB is also involved in specific reactions of the unsaturated fatty acid biosynthesis pathway. However, as the active site residues that seem to be of diagnostic value do not give a clear answer as well (36), the synthase is named PffabBF.

Sequence comparison further led to the identification of a number of highly conserved residues that constitute the active site. The configuration of the active site of all known elongation condensing enzymes is identical, containing a Cys/His/His catalytic triad (18, 37). In PffabBF, these residues are Cys-221, His-362, and His-399. We therefore assume

β -Ketoacyl-ACP Synthase from *P. falciparum*

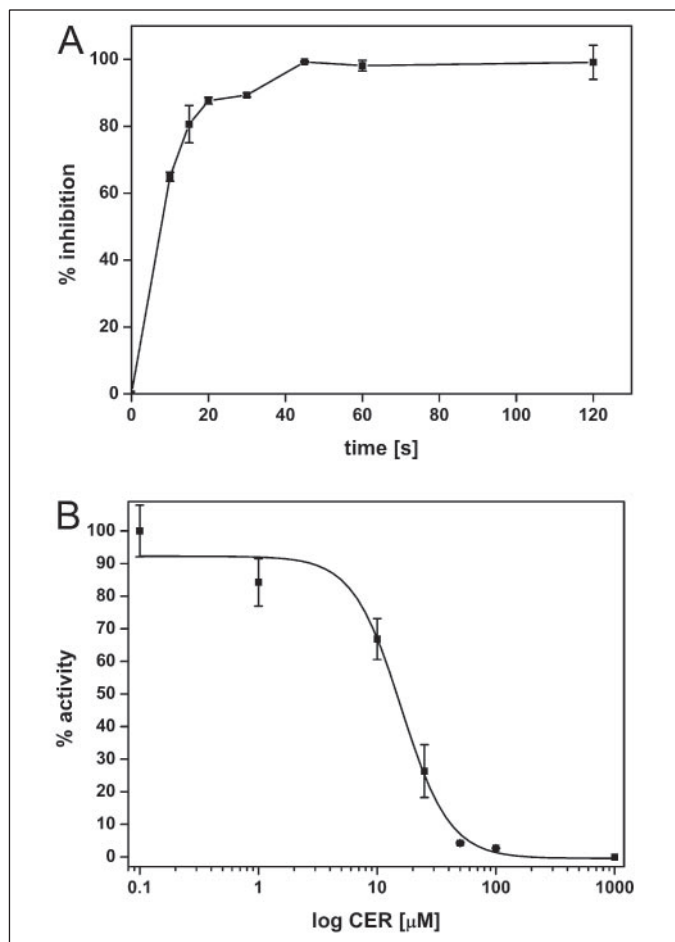


FIGURE 5. **PffabBF inhibition by cerulenin.** *A*, the effect of preincubation time on CER inhibition was examined by incubating the enzyme with 100 μM inhibitor for 10, 15, 20, 30, 45, 60, and 120 s prior to initiation of the reaction. *B*, the IC_{50} value was determined to be $15.8 \pm 2.3 \mu\text{M}$ under the conditions applied. The values were corrected for the remaining background activity, which is due to the fact that it takes 1 min until the enzyme is completely inactivated by CER (see *A*). The mean of duplicate measurements is shown.

that the PffabBF mechanism of acyl-enzyme formation, decarboxylation, and condensation is very similar to that of other organisms and that β -ketoacyl-ACP synthase inhibitors CER and TLM exhibit identical binding modes. Structural and biochemical analyses of PffabBF and its interaction with CER and TLM will be helpful in providing clues for the development of new compounds that selectively target PffabBF. We therefore established an expression system that allowed production of soluble and active PffabBF. Production of soluble protein was only achieved by expressing the NusA-PffabBF fusion protein under increased osmotic pressure (34, 35). It is assumed that subjecting the cells to osmotic stress by addition of sorbitol to the growth medium facilitates the uptake of the “compatible osmolyte” betaine. Betaine is believed to stabilize protein structure by minimizing solvent-protein contacts (35, 38).

PffabBF was assayed for activity with acyl-PfACP substrates as well as with the acyl-CoA derivatives to investigate chain length specificity of PffabBF for natural and artificial substrates. Acyl-PfACPs with chain lengths ranging from $\text{C}_{4:0}$ to $\text{C}_{16:0}$ were analyzed. PffabBF readily elongates $\text{C}_{6:0}$ - to $\text{C}_{10:0}$ -PfACP. The enzyme is significantly less active with $\text{C}_{4:0}$ -PfACP, and the catalytic efficiency decreases even more with the use of $\text{C}_{12:0}$ and $\text{C}_{14:0}$ -PfACP. Elongation of $\text{C}_{16:0}$ was not detected at all. The observed distribution of the catalytic efficiency indicates maximum PffabBF activity for $\text{C}_{6:0}$ -, $\text{C}_{8:0}$ -, and $\text{C}_{10:0}$ -PfACP substrates.

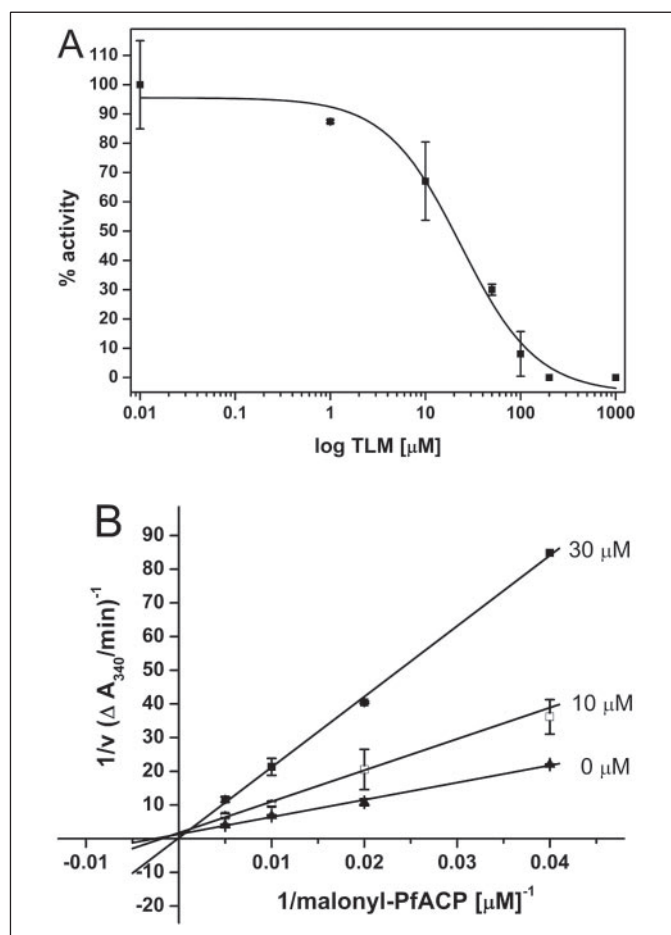


FIGURE 6. **PffabBF inhibition by TLM.** *A*, TLM inhibits PffabBF with an IC_{50} value of $23.6 \pm 6.0 \mu\text{M}$. *B* shows double-reciprocal plots of $1/v$ versus $1/[\text{malonyl-PfACP}]$. The lines intercept at the $1/v$ axis, indicating that TLM is a competitive inhibitor for malonyl-PfACP. A K_i of $10 \pm 4 \mu\text{M}$ was obtained.

Investigation of the kinetic parameters of the acyl-PfACP substrates revealed that the decreases in catalytic efficiency with $\text{C}_{12:0}$ and $\text{C}_{14:0}$ -PfACPs are caused by a slower conversion of the $[ES]$ complex to free enzyme and product ($E + P$) in the case of $\text{C}_{12:0}$ -PfACP and by a decreased affinity of the substrate for PffabBF in the case of $\text{C}_{14:0}$ -PfACP. $\text{C}_{12:0}$ has a K_m of 196 μM , which is in the range of the K_m values found for shorter chain acyl-PfACP. Here the lower catalytic efficiency is because of a lower V_{max} value. For $\text{C}_{14:0}$ -PfACP, an increase in K_m to 437 μM is observed, indicating a decreased affinity for the enzyme. $\text{C}_{10:0}$ -PfACP shows an interesting behavior; it is an efficient substrate despite a K_m of 403 μM , because of a high V_{max} value. These data are consistent with the recent analysis of parasite fatty acid synthesis using cell-free extracts. It was found that mainly C_{12} to C_{14} fatty acids were synthesized in *P. falciparum* (39).

We also tested the specific activities of PffabBF with acyl-CoAs. They are poor substrates with $\text{C}_{4:0}$ - to $\text{C}_{14:0}$ -CoAs being 100–150 times less active than the corresponding acyl-PfACPs. This is in agreement with the general observation that β -ketoacyl-ACP synthases exhibit low specific activity with acyl-CoA derivatives (16, 40). Surprisingly, among all acyl-CoAs tested, PffabBF displayed the highest activity for $\text{C}_{16:0}$ -CoA and $\text{C}_{18:0}$ -CoA. This is in direct contrast to the results obtained for the natural acyl-PfACP substrates that exhibit no activity with $\text{C}_{16:0}$ and $\text{C}_{18:0}$ acyl chain length. Investigation of the substrate acceptance of other β -ketoacyl-ACP synthases with a series of acyl-ACPs and the corresponding acyl-CoAs are not described in literature, and thus it is

not known whether this behavior is also common for other β -ketoacyl-ACP-synthases. However, as the activity of acyl-CoAs is very low and high substrate concentrations had to be applied, PfFabBF activity with respect to acyl-CoA is not likely to be physiologically relevant.

Given the very different substrate specificity of PfFabBF toward its natural and artificial substrates, it is likely that acyl-PfACPs and acyl-CoAs display different behavior also with the other enzymes involved in fatty acid biosynthesis. Thus, to avoid artifacts, acyl-PfACP should be used for characterizing enzymes in the *P. falciparum* type-II FAS system. This most probably also applies to FAS systems of other organisms.

Comparing the kinetic parameters of PfFabBF to the kinetic parameters of corresponding enzymes of other organisms is difficult due to different substrate specificities. For *M. tuberculosis* KasA and KasB with $C_{16:0}$ - and $C_{20:0}$ -ACP substrates (*E. coli*-ACP was used in this study), K_m values between 1.4 and 3.2 μM were reported, and thus the K_m values obtained for PfFabBF-substrates are about 100-fold greater than the ones reported for *M. tuberculosis* KasA and KasB (16). K_m values determined for *E. coli* FabB and FabF using $C_{14:0}$ -ACP (*E. coli*-ACP) are determined to be 71 and 68 μM , respectively. These results seem to be more in the range of the values determined for the corresponding substrates of PfFabBF. This is not surprising, because *E. coli* FabB and FabF exhibit substrate specificities that are similar to PfFabBF. In *E. coli*, the synthesis of $C_{14:0}$ and $C_{16:0}$ is predominant, but the specific activities of *E. coli* FabB and FabF with saturated acyl-ACPs are similar to the ones observed for PfFabBF (41, 42).

PfFabBF was tested for inhibition with CER and TLM. CER acts as a potent irreversible inhibitor of β -ketoacyl-ACP synthases by covalent modification of the active site cysteine thiol. As expected, PfFabBF was found to be very sensitive to CER. After 1 min of incubation with 100 μM CER, the enzyme was completely inactivated. This corresponds to a 10 times faster inactivation if compared with *M. tuberculosis* KasA and KasB. The k_{cat} values determined for PfFabBF were up to 36-fold higher than the k_{cat} values reported for the *M. tuberculosis* enzymes. The relatively high reactivity of PfFabBF could be an explanation for the rapid inactivation by CER.

TLM is known to inhibit β -ketoacyl-ACP synthases by competing with malonyl-ACP for binding (18, 19). We could show that this is also true for PfFabBF. As shown in Fig. 6B, the lines of the double-reciprocal plot intersect at the $1/\nu$ axis, indicating a competitive binding mode with respect to malonyl-PfACP. We obtained a K_i value of $10 \pm 4 \mu\text{M}$. Crystal structures of *E. coli* FabB in complex with TLM revealed that the O-3 of TLM forms strong hydrogen bonds with the two active site histidines (17). Because the mechanism of TLM binding to PfFabBF is identical to the one reported for other β -ketoacyl-ACP synthases, and because the His-His-Cys catalytic triad is highly conserved, we can assume that His-362 and His-399 of PfFabBF are involved in TLM binding.

All three β -ketoacyl-ACP synthases (FabB, FabF, and FabH) are susceptible to TLM inhibition but to a different extent. In *E. coli*, FabB is most inhibited by TLM, followed by FabF and FabH (17, 43). In *M. tuberculosis*, KasA is more sensitive to TLM than KasB (16). Thus, FabB seems to be the major target of TLM. The same is observed for the two β -ketoacyl-ACP synthases of *P. falciparum*; PfFabH is much less affected by TLM, with an IC_{50} of over 330 μM (21), compared with 23.6 ± 6 for PfFabBF.

The presented biochemical characterization of PfFabBF provides insight into the catalytic mechanism of PfFabBF. With the development of a system to produce soluble and active PfFabBF, it is now possible to extend the screening for inhibitors on the β -ketoacyl-ACP synthase activity of *P. falciparum*. Further investigation of the biochemical prop-

erties and structure of PfFabBF could form the basis for the rational design of new lead compounds.

Acknowledgments—We thank Dr. K. Otaguro (Research Center for Tropical Diseases, The Kitasato Institute, Japan) for providing thiolactomycin, Dr. T. Templeton (Weill Medical College of Cornell University) for providing the *P. falciparum* 3D7 cDNA library and MR4, and Dr. D. J. Carucci for providing the *P. falciparum* 3D7 gDNA.

REFERENCES

- Greenwood, B. M., Bojang, K., Whitty, C. J., and Targett, G. A. (2005) *Lancet* **365**, 1487–1498
- Hay, S. I., Guerra, C. A., Tatem, A. J., Noor, A. M., and Snow, R. W. (2004) *Lancet Infect. Dis.* **4**, 327–336
- Snow, R. W., Guerra, C. A., Noor, A. M., Myint, H. Y., and Hay, S. I. (2005) *Nature* **434**, 214–217
- Gardner, M. J., Hall, N., Fung, E., White, O., Berriman, M., Hyman, R. W., Carlton, J. M., Pain, A., Nelson, K. E., Bowman, S., Paulsen, I. T., James, K., Eisen, J. A., Rutherford, K., Salzberg, S. L., Craig, A., Kyes, S., Chan, M.-S., Nene, V., Shallom, S. J., Suh, B., Peterson, J., Angiuoli, S., Perlea, M., Allen, J., Selengut, J., Haft, D., Mather, M. W., Vaidya, A. B., Martin, D. M. A., Fairlamb, A. H., Fraunholz, M. J., Roos, D. S., Ralph, S. A., McFadden, G. I., Cummings, L. M., Subramanian, G. M., Mungall, C., Venter, J. C., Carucci, D. J., Hoffman, S. L., Newbold, C., Davis, R. W., Fraser, C. M., and Barrell, B. (2002) *Nature* **419**, 498–511
- Waller, R. F., Keeling, P. J., Donald, R. G., Striepen, B., Handman, E., Lang-Unnasch, N., Cowman, A. F., Besra, G. S., Roos, D. S., and McFadden, G. I. (1998) *Proc. Natl. Acad. Sci. U. S. A.* **95**, 12352–12357
- Waller, R. F., Ralph, S. A., Reed, M. B., Su, V., Douglas, J. D., Minnikin, D. E., Cowman, A. F., Besra, G. S., and McFadden, G. I. (2003) *Antimicrob. Agents Chemother.* **47**, 297–301
- Smith, S. (1994) *FASEB J.* **8**, 1248–1259
- Rock, C. O., and Cronan, J. E. (1996) *Biochim. Biophys. Acta* **1302**, 1–16
- Heath, R. J., White, S. W., and Rock, C. O. (2001) *Prog. Lipid Res.* **40**, 467–497
- Gornicki, P. (2003) *Int. J. Parasitol.* **33**, 885–896
- Roberts, C. W., McLeod, R., Rice, D. W., Ginger, M., Chance, M. L., and Goad, L. J. (2003) *Mol. Biochem. Parasitol.* **126**, 129–142
- Jones, A. L., Herbert, D., Rutter, A. J., Dancer, J. E., and Harwood, J. L. (2000) *Biochem. J.* **347**, 205–209
- Domergue, F., and Post-Beittenmiller, D. (2000) *Biochem. Soc. Trans.* **28**, 610–613
- Funabashi, H., Kawaguchi, A., Tomoda, H., Omura, S., Okuda, S., and Iwasaki, S. (1989) *J. Biochem. (Tokyo)* **105**, 751–755
- D'Agnolo, G., Rosenfeld, I. S., Awaya, J., Omura, S., and Vagelos, P. R. (1973) *Biochim. Biophys. Acta* **326**, 155–156
- Schaeffer, M. L., Agnihotri, G., Volker, C., Kallender, H., Brennan, P. J., and Lonsdale, J. T. (2001) *J. Biol. Chem.* **276**, 47029–47037
- Price, A. C., Choi, K.-H., Heath, R. J., Li, Z., White, S. W., and Rock, C. O. (2001) *J. Biol. Chem.* **276**, 6551–6559
- Heath, R. J., and Rock, C. O. (2002) *Nat. Prod. Rep.* **19**, 581–596
- Nishida, I., Kawaguchi, A., and Yamada, M. (1986) *J. Biochem. (Tokyo)* **99**, 1447–1454
- Kremer, L., Douglas, J. D., Baulard, A. R., Morehouse, C., Guy, M. R., Alland, D., Dover, L. G., Lakey, J. H., Jacobs, W. R., Jr., Brennan, P. J., Minnikin, D. E., and Besra, G. S. (2000) *J. Biol. Chem.* **275**, 16857–16864
- Jones, S. M., Urch, J. E., Brun, R., Harwood, J. L., Berry, C., and Gilbert, I. H. (2004) *Bioorg. Med. Chem.* **12**, 683–692
- Thompson, J. D., Desmond, G., Higgins, D. G., and Gibson, T. J. (1994) *Nucleic Acids Res.* **22**, 4673–4680
- Innis, M. A., Gelfand, D. H., Sninsky, J. J., and White, T. J. (eds) (1990) *PCR Protocols: A Guide to Methods and Application*, pp. 177–183, Academic Press Inc., San Diego
- Higuchi, R., Krummel, B., and Saiki, R. K. (1988) *Nucleic Acids Res.* **16**, 7351–7367
- Bradford, M. M. (1976) *Anal. Biochem.* **72**, 248–254
- Prigge, S. T., He, X., Gerena, L., Waters, N. C., and Reynolds, K. A. (2003) *Biochemistry* **42**, 1160–1169
- Waters, N. C., Kopydlowski, K. M., Guszczynski, T., Wei, L., Sellers, P., Ferlan, J. T., Lee, P. J., Li, Z., Woodard, C. L., and Shallom, S. (2002) *Mol. Biochem. Parasitol.* **123**, 85–94
- Heath, R. J., and Rock, C. O. (1996) *J. Biol. Chem.* **271**, 27795–27801
- Post-Beittenmiller, D., Jaworski, J. G., and Ohlrogge, J. B. (1991) *J. Biol. Chem.* **266**, 1858–1865
- Chopra, S., Singh, S. K., Sati, S. P., Ranganathan, A., and Sharma, A. (2002) *Acta Crystallogr. Sect. D Biol. Crystallogr.* **58**, 179–181
- Perozzo, R., Kuo, M., Sidhu, A. B. S., Valiyaveetil, J. T., Bittman, R., Jacobs, W. R., Jr., Fidock, D. A., and Sacchettini, J. C. (2002) *J. Biol. Chem.* **277**, 13106–13114
- Kissinger, J. C., Brunk, B. P., Crabtree, J., Fraunholz, M. J., Gajria, B., Milgram, A. J.,

β -Ketoacyl-ACP Synthase from *P. falciparum*

- Pearson, D. S., Schug, J., Bahl, A., Diskin, S. J., Ginsburg, H., Grant, G. R., Gupta, D., Labo, P., Li, L., Mailman, M. D., McWeeney, S. K., Whetzel, P., Stoeckert, C. J., and Roos, D. S. (2002) *Nature* **419**, 490–492
33. Waller, R. F., Reed, M. B., Cowman, A. F., and McFadden, G. I. (2000) *EMBO J.* **19**, 1794–1802
34. Makrides, S. C. (1996) *Microbiol. Rev.* **60**, 512–538
35. Blackwell, J. R., and Horgan, R. (1991) *FEBS Lett.* **295**, 10–12
36. Campbell, J. W., and Cronan, J. E. (2001) *Annu. Rev. Microbiol.* **55**, 305–332
37. McGuire, K. A., Siggaard-Andersen, A. M., Bangera, M. G., Olsen, J. G., and von Wettstein-Knowles, P. (2001) *Biochemistry* **40**, 9836–9845
38. Arakawa, T., and Timasheff, S. N. (1985) *Biophys. J.* **47**, 411–414
39. Surolia, N., and Surolia, A. (2001) *Nat. Med.* **7**, 167–173
40. D'Agnolo, G., Rosenfeld, I. S., and Vagelos, P. R. (1975) *J. Biol. Chem.* **250**, 5283–5288
41. Edwards, P., Sabo Nelsen, J., Metz, J. G., and Dehesh, K. (1997) *FEBS Lett.* **402**, 62–66
42. Garwin, J., Klages, A., and Cronan, J., Jr. (1980) *J. Biol. Chem.* **255**, 3263–3265
43. Tsay, J. T., Rock, C. O., and Jackowski, S. (1992) *J. Bacteriol.* **174**, 508–513